ELSEVIER

Biochimica et Biophysica Acta 1369 (1998) 309–319

BIOCHIMICA ET BIOPHYSICA ACTA
BBA

Alamethicin-like behaviour of new 18-residue peptaibols, trichorzins PA. Role of the C-terminal amino-alcohol in the ion channel forming activity

Delphine Duval [a], Pascal Cosette [b], Sylvie Rebuffat [a], Hervé Duclohier [b], Bernard Bodo [a], Gérard Molle [b,*]

[a] *Laboratoire de Chimie des Substances Naturelles, URA 401 CNRS, GDR 1153 CNRS, IFR 63 CNRS-INSERM, Muséum National d'Histoire Naturelle, 63 rue Buffon, 75231 Paris Cedex 05, France*
[b] *Laboratoire ''Polymères, Biopolymères, Membranes'', UMR 6522 CNRS, GDR 1153 CNRS, IFRMP 23, Université de Rouen, 76821 Mont-Saint-Aignan, France*

Received 16 July 1997; revised 23 September 1997; accepted 24 September 1997

Abstract

The influences of peptide length, absence of a Glx (Gln/Glu) residue and the C-terminal amino alcohol on liposome permeabilization and ion-channel characteristics in planar lipid bilayers were examined with two 18-residue peptaibols, PA V and PA IX. As compared to the 20-residue alamethicin, both peptides belonging to the newly isolated trichorzin family, lack a proline in the N-terminal part and one of the two Gln/Glu residues in the C-terminal part of the sequence. The two analogues studied here differ among themselves in their C-terminal amino alcohol (tryptophanol for PA V and phenylalaninol for PA IX). These α-helical peptaibols modify to a similar extent the permeability of liposomes, as measured by leakage of a previously entrapped fluorescent probe. Monitoring tryptophanol fluorescence, a greater embedment of the peptide PA V is observed in cholesterol-free bilayers. Macroscopic conductance studies for PA V and PA IX display alamethicin-like current–voltage curves, with a similar voltage dependence, but a smaller mean number of monomers per conducting aggregate is estimated for the tryptophanol analogue, PA V. Single-channel recordings indicate faster current fluctuations for PA IX, while amplitude histograms show lower conductance levels for PA V. Apart from underlining the role of the mismatch between helix length and bilayer hydrophobic thickness, these results stress that the C-terminal tryptophanol favours a stabilization of the conducting aggregates. © 1998 Elsevier Science B.V.

Keywords: Pore formation; Peptaibol; Tryptophan; Fluorescence; Lipid bilayer; Voltage-dependent conductance

1. Introduction

Trichorzins PA (PA II, PA IV–IX) are 18-residue peptides isolated from the fungus *Trichoderma harzianum* [1]. They are characterized by a high proportion of α-aminoisobutyric acid (Aib) and isovaline (Iva), an N-terminus protected by an acetyl group and a C-terminal amino alcohol. They thus belong to the peptaibol class of antibiotics [2,3], of which the 20-residue alamethicin [2] is the most extensively studied. The seven recently isolated trichorzins PA have been shown to differ among themselves in Aib for Iva substitutions at positions 4 and 7, and tryptophanol (Trpol) for phenylalaninol (Pheol)

* Corresponding author. Fax: +33 235 14 6704; E-mail: gerard.molle@univ-rouen.fr

PII S0005-2736(97)00235-6

replacements at the C-terminus. Both kinds of modification only result in slight variations of the global hydrophobicity and do not perturb the α-helical structure determined for these peptides [1].

Peptaibols are classified into three main subclasses according to their chemical characteristics and amino acid chain length:

(i) the long-sequence peptaibols [4–7] with 18–20 residues including trichorzins PA and alamethicins;
(ii) the short-sequence peptaibols such as zervamicins [8] or harzianins [9,10], with 11–16 residues and characterized by the presence of several Aib–Pro–Xaa–Xaa motives; and
(iii) the lipopeptaibols with 7–11 residues, a high content in glycines and an N-terminus acylated by a short saturated [11,12] or unsaturated lipid chain [13].

Biosynthesized by microscopic saprophytes fungi which assure the destruction of organic scraps and exert a biological control of soils, peptaibols have been shown to inhibit the growth of various microorganisms such as bacteria, fungi and parasites. We recently found that trichorzins PA exert a potent activity against various strains of mycoplasma and spiroplasma [1]. The antibiotic properties exhibited by peptaibols are also shown to be related to the membrane perturbation and/or ion-channel formation. It is generally admitted that alamethicin induces ion channels in lipid bilayers by formation of conducting aggregates, each made up of several helical peptide monomers. The characteristic conductance properties, a set of transitions between non-integral subconductance states, result from uptake and release of monomers inside the aggregate, according to the barrel-stave model [14,15] (for reviews, see Refs. [16,17]).

In previous papers [18–21], we studied the channel-forming properties of long- and short-sequence natural Aib-containing peptides. It was found that the 19- and 20-residue analogues of alamethicin display similar membrane-channel activity pattern, in agreement with the above-mentioned model [18–20]. Though also forming channels made of peptide helix aggregates, the shorter 14-residue harzianins HC exhibit a different behaviour, presumably involving pores made of a fixed number of monomers [21]. In this contribution, we study the interaction of two trichorzins PA (sequences shown in Fig. 1) with phospholipids in order to determine their embedment in the bilayer, and describe their conductance properties. We point to an alamethicin-like behaviour of these peptides and examine the role of either Trpol or Pheol as C-terminal amino alcohol in the channel stabilization.

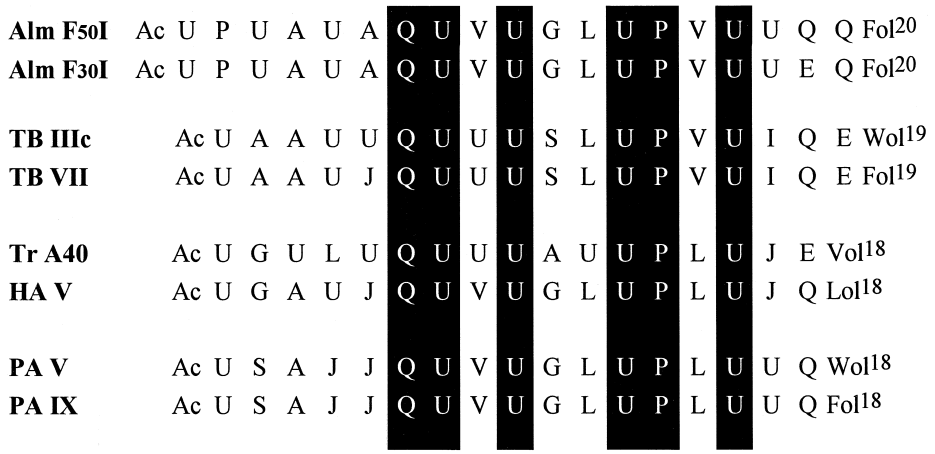

Fig. 1. Amino acid sequences of neutral and charged alamethicins (Alm F_{50I} and Alm F_{30I}), trichorzianins (TB IIIc and TB VII), trichotoxin A_{40} (TrA40) and trichorzins HA V compared with the presently-studied PA V and PA IX. One letter code (U – α-aminoisobutyric acid, J – isovaline, Fol – phenylalaninol, Wol – tryptophanol, Vol – valinol and Lol – leucinol). In shaded areas: absolutely conserved residues.

2. Materials and methods

2.1. Isolation and characterization of trichorzins PA

Trichorzins PA were isolated from *Trichoderma harzianum* (strain M-902608, Muséum National d'Histoire Naturelle) by a multistep chromatography procedure, including semi-preparative HPLC (Kromasil C18 5 μm, 7.5 × 300 mm, AIT, France) with MeOH/H_2O (84/16, v/v) as eluent at a flow rate of 2 ml/min. UV detection was at 220 nm and retention times R_t (in min) were: 74, 89, 95, 106, 111, 127 and 134 for PA II, PA IV, PA V, PA VI, PA VII, PA VIII and PA IX, respectively. The sequences of trichorzins PA II and PA IV-IX have been determined by mass spectrometry and two-dimensional nuclear magnetic resonance and their helical conformation issued from NOE data [1].

2.2. Circular dichroism

The CD spectra of trichorzins PA V and PA IX were recorded in methanol solutions on a Mark V Jobin Yvon dichrograph (0.12 mM, 0.1 mm pathlength cell, $T = 23°C$). Blanks obtained in the same conditions were subtracted. The experimental curves were obtained from 51 ellipticity values from 190 to 240 nm. Peaks and throughs characteristic wavelengths (λ, in nm) and associated mean residue ellipticities ($[\theta]$M (deg cm^2 dmol^{-1}) were as follows: PA V: 193 (608 000), 208 (−208 500), 223 (−171 500); PA IX:193 (910 200), 208 (−332 600), 223 (−265 600).

2.3. Preparation of small unilamellar vesicles (SUV) and carboxyfluorescein (CF)-entrapped SUV

Egg phosphatidylcholine (ePC type V-E), KI and $Na_2S_2O_3$ were purchased from Sigma and used without further purification; cholesterol (Chol) from Sigma was recrystallized from methanol. Carboxyfluorescein (CF) from Eastman Kodak was cleared from hydrophobic contaminants and recrystallized from ethanol, as previously described [20]. SUV were prepared by sonication (Ultrasonics Model W-225 R) to clarity of a 0.5 mM solution of either egg PC or egg PC/Chol (7/3) in 1 mM NaCl, 0.2 mM EDTA, 1 mM cacodylate buffer (pH 7.20), at 0°C under nitrogen for 45 min. CF-entrapped SUV were prepared by sonication of a 8.5 mM solution of egg PC/Chol (7/3), in 56 mM CF, 1 mM NaCl, 5 mM Hepes buffer (pH 7.42), at 0°C under nitrogen for 20 min. The unencapsulated CF was removed by gel chromatography through Sephadex G75 column (1 × 25 cm) eluted with the above-mentioned buffer and the dilution factor determined.

2.4. Fluorescence measurements on liposomes

Fluorescence spectra were obtained at 20°C on an Aminco/SPF500 spectrofluorometer from peptides in methanolic solutions, the methanol final concentrations being kept below 0.5% (by volume). For tryptophan fluorescence measurements, 5 μl of a 0.25 mM methanolic trichorzin PA V solution were added to the freshly prepared SUV suspension diluted in the above-mentioned cacodylate buffer (pH 7.2) in order to give $R_i = [lip]/[pep]$ ratios in the 0–200 range, with a constant 0.89 μM peptide concentration. Emission spectra were recorded between 200 and 500 nm (5 nm band pass) with λ_{exc} at 280 nm (4 nm band pass) after a 15 min period of incubation and were corrected from the vesicular emission. For quenching measurements, 30 μl of 0.7–10 M KI and 0.1 mM $Na_2S_2O_3$ solutions were added to 9×10^{-7} M solutions of PA V in either 1400 μl of cacodylate buffer or 125 μl SUV suspension in 1275 μl cacodylate buffer ($R_i = [lip]/[pep] = 50$), at constant ionic strength by addition of NaCl. Emission spectra were recorded after 10 min incubation. The values (averaged for five measurements) were corrected for the scatter contribution derived from a KI titration of a vesicle blank.

For permeabilization measurements, aliquots of methanolic peptide solutions were added to a mixture of 200 μl vesicular suspension and 1200 μl of 5 mM Hepes buffer (pH 7.42). The peptide concentrations were calculated to give $R_i^{-1} = [pep]/[lip]$ values ranging between 0 and 3×10^{-3}. The kinetics ($\lambda_{exc} = 488$ nm, $\lambda_{em} = 520$, 1 nm band pass) were monitored after rapid stirring and stopped at 20 min; a 50 μl amount of Triton X-100 (10% in H_2O) was added to disrupt the SUV and determine the total fluorescence (F_T). Percentages of released CF at 20 min were determined as $(F_{20} - F_0)/(F_T - F_0) \times$

100, with F_0 and F_{20} representing the fluorescence intensities in the absence of peptide, and at 20 min in the presence of peptide, respectively.

2.5. Macroscopic and single-channel conductance experiments in planar lipid bilayers

Lipids, 1-palmitoyl 2-oleoyl phosphatidylcholine (POPC) and 1,2-dioleoyl phosphatidylethanolamine (DOPE), were purchased from Avanti Polar Lipids (Alabaster, AL) and stored at −74°C. For both kinds of experiment, the lipid mixture was POPC/DOPE (7/3, w/w). In macroscopic current measurements, virtually solvent-free lipid bilayers were formed over a 150 μm hole in a 10 μm-thick PTFE (Goodfellow, Cambridge, UK) septum sandwiched between two half-glass cells. An aliquot of 5 μl lipid solution at 10 mg/ml was spread on the top of electrolyte solutions (1 M KCl, 10 mM Hepes, pH 7.4) in both compartments. Bilayer formation was achieved by lowering, and then raising the electrolyte level in one or both sides according to the Montal and Mueller technique [22]. In single-channel experiments, lipid bilayers were formed at the tip of fire-polished patch-clamp pipettes according to the 'tip-dip' method [23]. Briefly, 10 μl of a lipid solution in hexane (0.5 mg/ml) were spread on the surface of a glass cell filled with 2 ml of 1 M KCl. The fire-polished hard-glass pipette, filled with a solution of 1 M KCl and 1 mM $CaCl_2$ in order to favour the seal, was withdrawn and then slowly dipped again in order to form the bilayer. Thereafter, 6 μl of 1 μM methanol peptide stock solution were added into the *cis*-side compartment. A patch-clamp amplifier (Bio-Logic, Claix, France) was used to record single-channel currents. The latter were fed to an eight-pole Bessel filter and stored on a digital tape recorder (respectively, AF 180 and DTR 1200 models from Bio-Logic). Digitized signals were subsequently analyzed using the Satori V3.01 software from Intracell (Royston, UK).

3. Results

3.1. Interaction of trichorzins PA with small unilamellar vesicles (SUV)

The trichorzin/bilayer interaction was studied by fluorescence spectroscopy, using the C-terminal tryptophanol fluorophore of trichorzin PA V as an intrinsic probe. Addition of egg PC vesicular suspension to a cacodylate buffer solution of PA V for R_i = [lip]/[pep] values up to 150 resulted in a 25 nm blue shift of the fluorescence maximum wavelength from 355 to 330 nm (Fig. 2A), accompanied by a concomitant increase in the fluorescence intensity (Fig. 2B). The presence of 30% cholesterol in the SUV did not appear to seriously affect the fluorescence changes; it only reduced the wavelength shift to 20 nm. The R_{iB} values determined from the intercept of the linear part of the binding curve and the plateau represent the minimum number of phospholipid molecules required for the binding of one peptide and, thus, characterize the peptide/bilayer interaction. These values are quite close for pure ePC ($R_{iB} = 70$) and

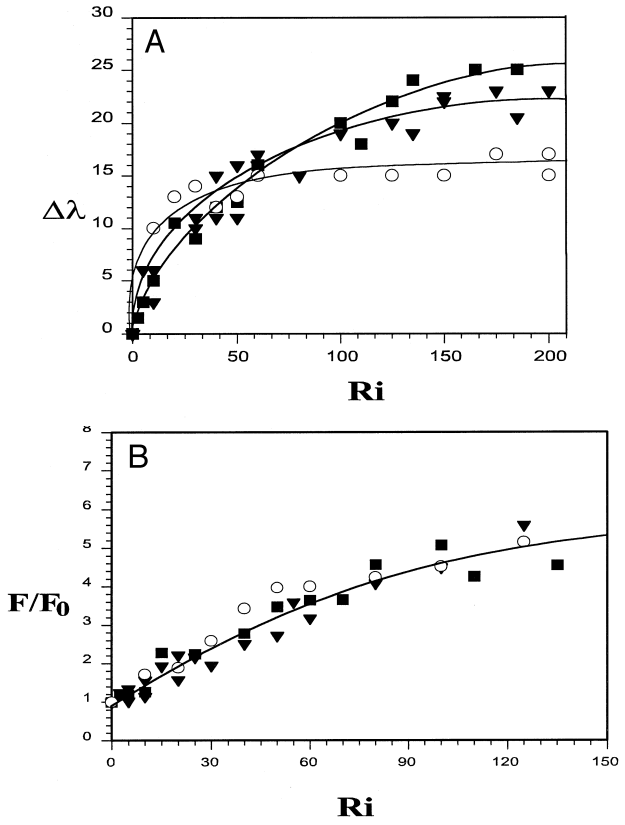

Fig. 2. (A) Emission wavelength blue shift from 355 nm ($\Delta\lambda$) and (B) relative increase in the fluorescence intensity (F/F_0) at 335 nm as a function of [lip]/[pep] molar ratios (R_i) for (○) tryptophan octyl ester (TOE)/ePC, (■) PA V/ePC and (▼) PA V/ePC:Chol (7:3). λ_{exc} = 280 nm and T = 20°C. TOE was used as a simple model for a hydrophobic chain bearing a tryptophan head.

ePC/Chol 7/3 bilayers ($R_{iB} = 80$). The observed fluorescence modifications, characteristic of an increase in the hydrophobicity of the Trpol microenvironment, could thus be interpreted by the incorporation of trichorzin PA V into the phospholipid bilayer.

3.2. Quenching measurements

Iodide, a large polar anion, is a collisional quencher thought to have access only to surface-exposed Trp residues and is useful in determining the extent of solvent accessibility of a Trp residue. More direct information about the localization and accessibility of the C-terminal Trpol residue of trichorzin PA V was thus obtained by studying the influence of I^- on the fluorescence intensity. Addition of potassium iodide to a solution of trichorzin PA V resulted in a decrease in the fluorescence intensity, corresponding to the fluorophore fraction available to the quencher (f_a), and the accessibility of the fluorophore was calculated using modified Stern–Volmer plots [24,25] (Fig. 3). In the absence of lipids, f_a was 100%, in agreement with a total accessibility of the C-terminal Trpol to the quencher. After adding ePC SUV, the Trpol accessibility was reduced to 30%, suggesting the embedment of the peptide into the bilayer. The f_a value measured in ePC/Chol 7/3 SUV was 90%, thus indicating a greater exposure of the Trpol to the aqueous phase.

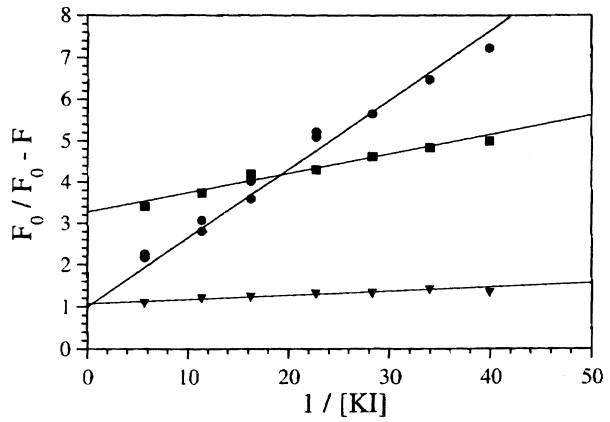

Fig. 3. Modified Stern–Volmer plot for the I^- quenching of the PA V Trpol fluorescence. The experiments were carried out by adding 30 μl of 0.7 to 10 M KI solutions to a PA V solution, in (●) the absence or presence (■) of ePC or (▼) ePC/Chol 7:3 vesicles. $R_i = 50$ and $\lambda_{exc} = 280$ nm. Data were analyzed, according to the Lehrer-modified Stern–Volmer relationship $F_0/\Delta F = 1/[Q]f_a K_{sv} + 1/f_a$, where F_0 is the fluorescence intensity in the absence of quencher, ΔF the difference of fluorescence intensity in the absence, and in the presence of quencher, $[Q]$ the quencher concentration and f_a the fraction of total fluorescence available to the quencher. $K_{sv} = \tau_o\ k$ was the Stern–Volmer quenching constant with τ_o the lifetime of the excited state, and k the rate constant for the deactivation of the fluorophore by the quencher [24]. f_a values were determined by interpolation to 0 of the $F_0/\Delta F$ vs. 1/[KI] plots.

3.3. Permeabilization measurements

Membrane permeabilization induced by trichorzins PA V and PA IX is an indirect proof of the interaction of both trichorzins with lipid bilayers [6,21,26]. This was followed by monitoring the leakage of the fluorescent probe, carboxyfluorescein (CF), entrapped in ePC/Chol (7:3) vesicles at a self-quenched concentration [27]. Different [peptide]/[lipid] ratios (R_i^{-1}) were assayed for CF release and fluorescence dequenching upon dilution in the external medium. The [lipid]/[peptide] ratios resulting in 50% leakage in 20 min of the entrapped probe (R_{i50}) were taken as a measure of the peptide efficiency. Integrity of the vesicles over the course of the leakage was verified by checking the absence of modification of the scattering peak intensity at 488 nm. Both trichorzins exhibited the same R_{i50} value of 1670 reflecting a strong permeabilization of ePC/Chol liposomes.

3.4. Functional assays: Macroscopic current measurements

Peptides, added to the *cis*-side, were incorporated into POPC/DOPE (7/3) bilayers, formed according to the Montal–Mueller technique [22]. Typically, after 30 min, the bilayer was submitted to repetitive triangular voltage ramps. Current–voltage (I/V) curves were recorded and superimposed, ensuring that partitioning equilibrium between peptide and membrane was reached. An exponential development of membrane current above a voltage threshold was observed for trichorzins PA V and PA IX, in agreement with the typical alamethicin-like behaviour. The macroscopic I/V curves, recorded for the same concentration of both peptides showed a lower threshold value of 120 mV for exponential branches for PA IX

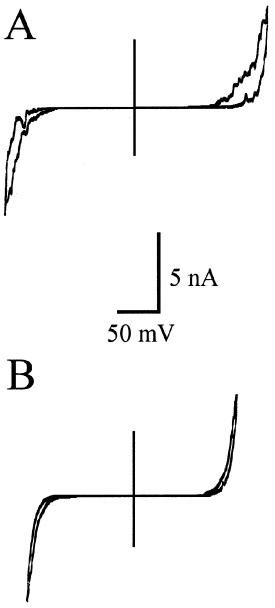

Fig. 4. Macroscopic I/V curves obtained for similar (1.5×10^{-8} M) concentrations of (A) PA V and (B) PA IX in DOPC/DOPE (7/3) bilayers bathed with 10 mM Hepes, 1 M KCl buffer (pH 7.4, room temperature). The curves were recorded half an hour after the peptide addition into the *cis*-side compartment.

as compared to PA V (160 mV) (Fig. 4). To estimate the channel kinetics at the macroscopic level, bilayers were submitted to strictly identical voltage sweeps of 20 mV/s. In such conditions, PA V channels remained open for a longer period (Fig. 4), as indicated by a broader hysteresis in agreement with further observations at the single-channel level (see in the following).

As previously demonstrated for alamethicin [28], the evolution of the I/V curves with the peptide concentration (Fig. 5) allows to estimate a mean number of monomers per conducting aggregate, N_{app}, as V_a/V_e. In our experiments, V_e – the voltage shift resulting in an e-fold change in conductance – was similar for both peptides, while major difference appeared for the V_a – the threshold shift for an e-fold change in concentration – which was lower for the Trpol-bearing peptide (Table 1). A different mean number of monomers was thus involved in the channel formed by the two trichorzins, this number being much more reduced for PA V (Table 1).

The I/V curves obtained for PA V and PA IX were symmetrical (Fig. 4), as previously observed for neutral trichorzianin TA IIIc [18] or saturnisporin SA IV [18] and contrasting with the negatively charged trichorzianin TB IIIc [19] and F30 alamethicin [28]. Such a behaviour could be due to fast reorientation of helix dipoles upon applying the voltage, favoured by

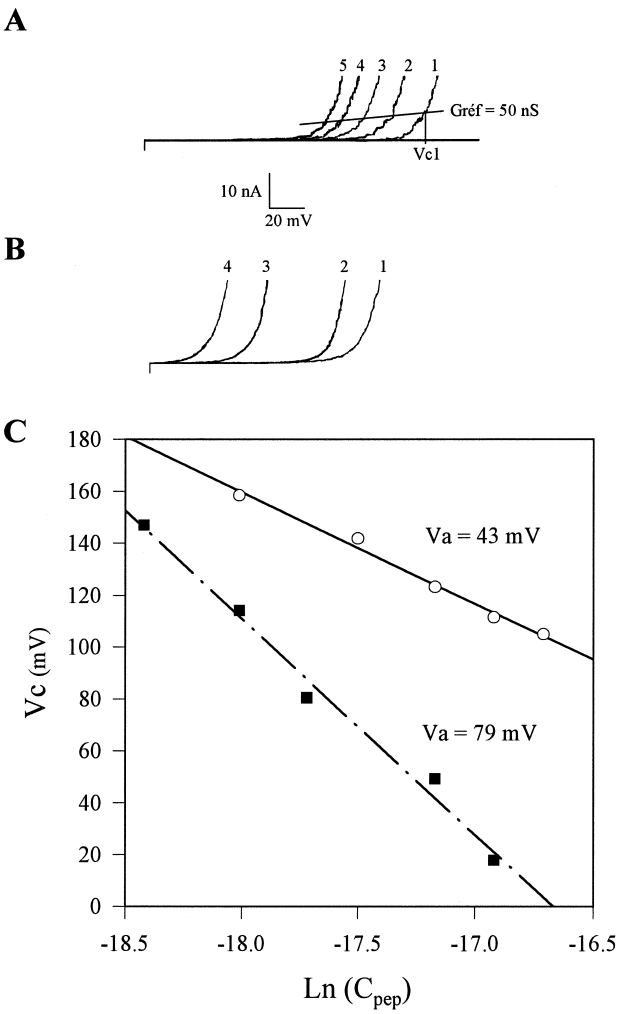

Fig. 5. Macroscopic current–voltage curves obtained for different peptide concentrations of PA V and PA IX in POPC/DOPE (7/3) bilayers bathed with 10 mM hepes, KCl 1 M (pH 7.4, room temperature). (A) PA V, 1.5×10^{-8} M (curve 1); 2.5×10^{-8} M (curve 2); 3.5×10^{-8} M (curve 3); 4.5×10^{-8} M (curve 4); and 5.5×10^{-8} M (curve 5). (B) PA IX 10^{-8} M (curve 1); 2×10^{-8} (curve 2); 3.5×10^{-8} M (curve 3) and 4.5×10^{-8} M (curve 4). For each concentration, the curves are averaged over 10 to 20 I/V sweeps. (C) Concentration dependence of macroscopic currents compared for PA V (○ – solid line) and PA IX (■ – dotted line). The evolution of the characteristic voltage V_c (for a reference conductance $G = 50$ nS, see part A of the figure) as a function of peptide concentration allows the calculation of the slope V_a, the voltage shift of thresholds resulting from an e-fold change in peptide aqueous concentration.

Table 1
Macroscopic conductance parameters for trichorzins PA V and PA IX. Concentration- and voltage-dependences, V_a and V_e, are given ± 5 mV and ± 1 mV, respectively. Resulting number of monomers per channel (N_{app}) are rounded and given ± 1

	V_a (mV)	V_e (mV)	N_{app}
PA V	43	8.5	5.0
PA IX	79	8.5	9.0

Table 2
Statistical analysis of single-channel recordings for PA V at 160 mV and PA IX at 145 mV. The different states observed are given by C closed, O_1 first open state, etc... γ Values are the conductance levels for each open state. P_o are the probabilities of being on a given level at the applied voltage. τ Values are the mean open times of the different states. The data are averaged over more than 100 000 events for each peptides. Experimental conditions are as given in legend of Fig. 6

		C	O_1	O_2	O_3	O_4
PA V	γ (pS)	—	145	515	1115	1740
	P_o	0.25	0.43	0.26	0.05	< 0.01
	τ (ms)	1.08	0.84	0.71	0.50	0.42
PA IX	γ (pS)	—	270	735	1535	2355
	P_o	0.23	0.46	0.25	0.06	< 0.01
	τ (ms)	1.03	0.61	0.45	0.34	0.25

the absence of formal electrical charge, in agreement with previous studies which showed that I/V curves became symmetric when blocking the N-terminus or the Glu negative charge near the C-terminus by Boc and benzyl groups, respectively [28].

3.5. Functional assays: Single-channel conductance

The trends revealed in the macroscopic analysis were confirmed at the single-channel level. As no discrete conductance events could be resolved at room temperature, these experiments were conducted at 10°C and bilayers formed at the tip of patch pipettes. In these conditions, both peptides induced

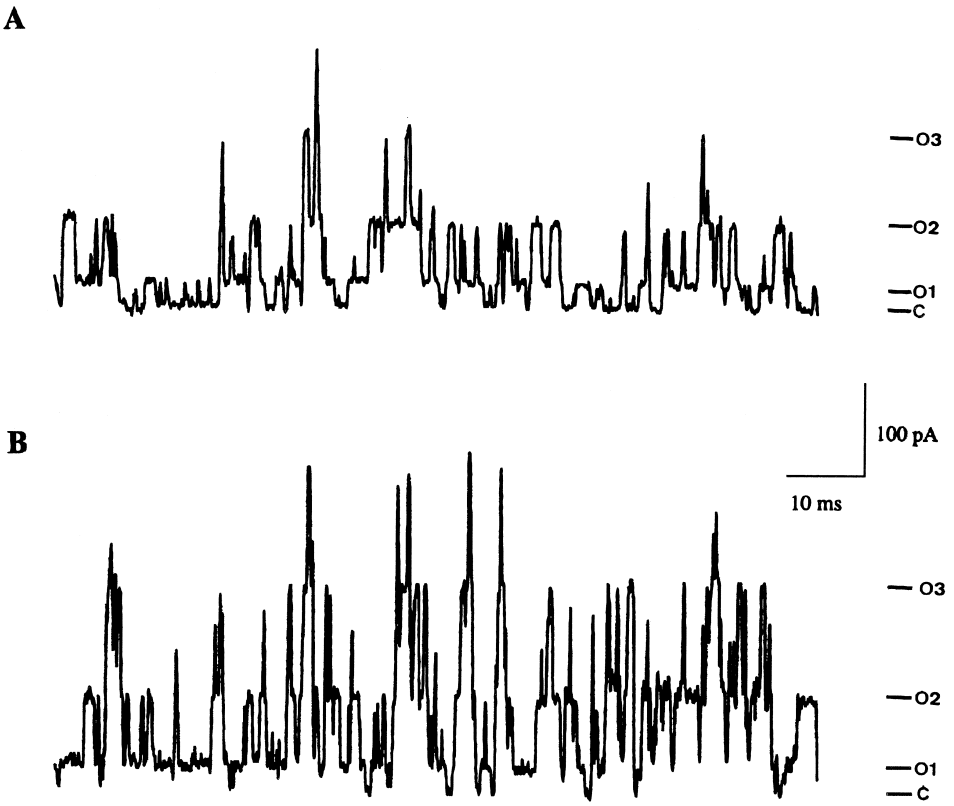

Fig. 6. Single channel fluctuations induced by trichorzins PA V and PA IX into POPC/DOPE (7/3) bilayers in 1 M KCl solutions at the tip of patch-clamp pipettes and at 10°C. Bessel filter was set to 10 KHz and data were digitized at 25 KHz for computer analysis. (A) PA V, 3.10^{-9} M, V = 160 mV and (B) PA IX, 3.10^{-9} M, V = 145 mV. (C – closed state; O_1 – 1st open substate, O_2 – 2nd open substate,...).

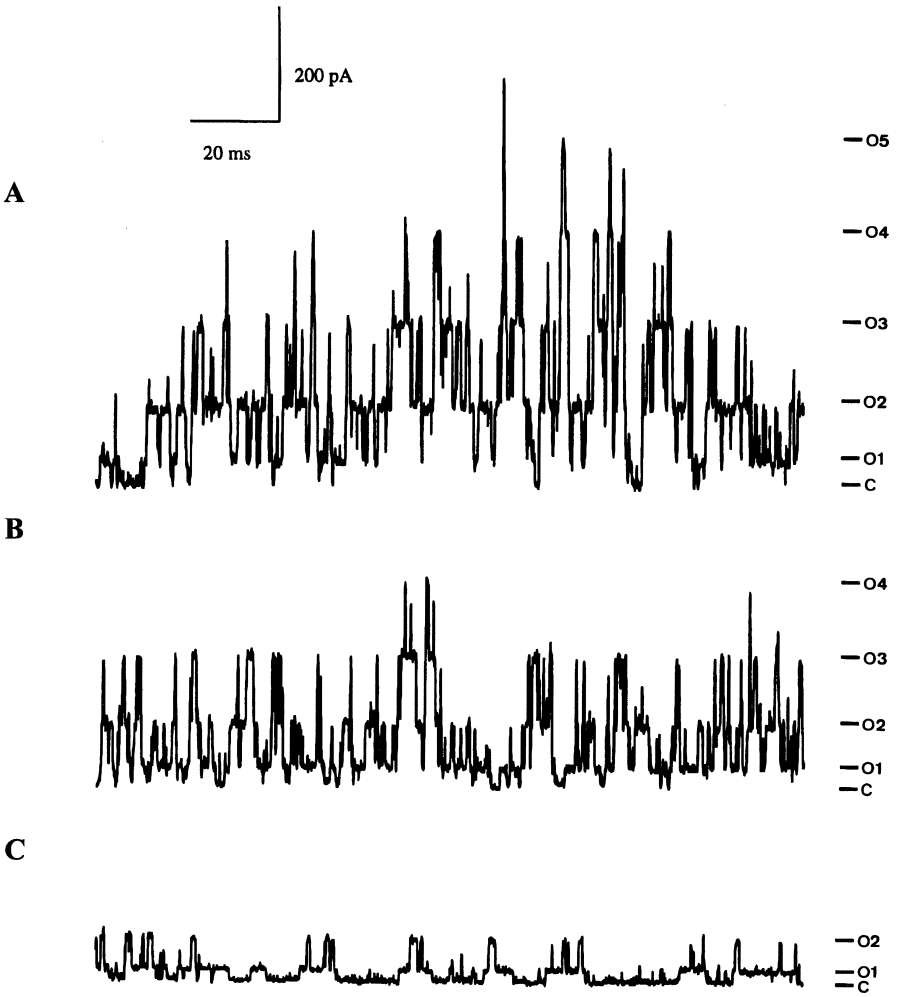

Fig. 7. Voltage-dependent behaviour for trichorzin PA IX in single-channel experiments at three different applied voltages. (A) 185 mV, (B) 145 mV and (C) 120 mV. Other experimental conditions are similar to those described for Fig. 6.

the multi-state behaviour first characterized for alamethicin (Fig. 6). The different subconductance levels with non-integral increments (Table 2) are in agreement with the barrel-stave model, the fluctuations between substates being correlated with the uptake and release of helical monomers in the bundle [14–17].

The conductance values observed for the four first levels indicated lower conductance levels for PA V, as compared to PA IX. Although probabilities for the different open substates were similar in both cases, the lifetimes were larger ($\times 1.5$) in the former analogue, PA V (Table 2). This confirms the analysis of the I/V curves, whose broader hysteresis for PA V (Fig. 4) also points to longer channel durations.

Table 3
Probabilities (P_o) observed for the different states (C, O_1, O_2, O_3, O_4) induced by Pa IX at different voltages. The values presented here are extracted from different recordings which are composed of ~500 000 events. For each voltage, the number in bold is for the state with the highest probability. Experimental conditions are as given in legend of Fig. 6

State	Conductance (pS)	P_o			
		90 mV	120 mV	145 mV	185 mv
C	—	**0.68**	**0.58**	0.23	0.07
O_1	270	0.28	0.35	**0.46**	0.29
O_2	735	0.04	0.06	0.25	**0.43**
O_3	1535	ND *	< 0.01	0.06	0.18
O_4	2355	ND *	ND *	< 0.01	0.03

* Not determined

Finally, the voltage dependence of the probabilities of the different open states was examined in the case of trichorzin PA IX (Fig. 7, Table 3). At lower voltages (90 and 120 mV), the closed state C was the more frequent level and the probability of the open substate O_2 was very low. Increasing the voltage gradually favours upper levels, as the first O_1 and the second O_2 open substates were the most frequently observed states at 145 mV and 185 mV, respectively (Table 3). It thus appears that larger voltages result in further monomer incorporation into the conducting aggregates.

4. Discussion

Compared to the longer alamethicin [29,30], both 18-residue peptaibols trichorzins PA adopt a similar overall helical conformation, as shown here by ellipticities and as studied earlier by NMR in methanol solution [1], a medium in which peptaibols have been shown to display a structure close to that in phospholipid bilayers [31]. The α-helical structure includes a bend stabilized by two 3_{10} turns ($4 \rightarrow 1$ bond) in the 11–15 region containing the proline residue. The helix lengths of trichorzins and alamethicin should, thus, be ≈ 30 Å and 33 Å, respectively. Such values would allow both peptide types to span the hydrocarbon core of a bilayer, the 18-residue peptaibol length being however very close to the average 30 Å thickness of a bilayer.

In the present study, we have shown that, in the absence of voltage, trichorzins PA V and PA IX interact with phospholipid bilayers of liposomes in the 0.1–1 μM range and perturb their permeability to the same extent. The Trpol-containing peptide, trichorzin PA V, was embedded into the bilayer with its C-terminus near the polar heads of phospholipids. When 30% cholesterol was added in the bilayer, this embedment was reduced, an effect previously noticed with the longer 19-residue trichorzianins [25]. The liposome permeabilization ability of both trichorzins, as expressed by R_{i50} values, was in the range usually found for related long-sequence peptaibols, also interacting with zwitterionic bilayers by a mechanism mainly governed by hydrophobic effects [6,21,26]. Overall, these data indicate that the replacement of a C-terminal Trpol for a Pheol does not result in significant changes in peptide/liposome interactions.

In planar lipid bilayers, trichorzins PA V and PA IX are also shown here to form voltage-gated ion channels according to the barrel-stave model, i.e. conducting aggregates of transbilayer helices with uptake and release of individual monomers. Indeed, the conductance values of the substates are not integral multiples of a unit-conductance step but increase in geometrical progression, a typical behaviour first described for alamethicin, the prototypic 20-residue peptaibol [15]. However, such discrete conductance levels could only be resolved when decreasing the temperature down to 10°C. As previously observed with harzianin HA V, another 18-residue peptaibol bearing a C-terminal leucinol [20], single-channel experiments conducted at room temperature with trichorzins PA V and PA IX resulted in very fast current fluctuations, suggesting an inadequate helix length and bilayer thickness. Similarly, trichotoxin TrA40 (sequence shown in Fig. 1), another 18-residue long peptaibol, has also been shown to induce short-lived discrete current levels as described in a pioneering work by Boheim et al. [32]. In a subsequent report by the same group [33], a major role for the [Gln–Gln] or [Glu–Gln] cluster near the C-terminus was suggested in order to explain the bursting behaviour of the 18-residue trichotoxin A40. The latter lacks one of these two residues which are prone to form inter-helix H-bonds. However, the 19-residue trichorzianins which contain the above-mentioned cluster also require a temperature decrease and a special lipid mixture to form well-resolved conductances [19]. In addition, two synthetic alamethicin analogues, in which all Aib residues were replaced by Leu, were shown to form ion channels with similar kinetics [34] whether or not Glu18 is included in the sequence. Altogether, comparison of channel kinetics induced by 20-, 19- and 18-residue peptaibols suggests a parallel reduction of substates lifetimes with the sequential deletion of a residue in the C-terminal part.

The conductance properties exhibited by trichorzins PA V and PA IX appear appreciably different as regards mean numbers of monomers on one hand, and single-channel amplitudes and kinetics on the other. Despite the two kinds of experiment being carried out at different temperatures, the higher N_{app}

found with PA IX is at least qualitatively in agreement with the single-channel data. Indeed, if the open probabilities of the different substates for both analogues appear similar (Table 2), they were obtained at slightly different voltages. Taking into account the voltage dependence of the substates shown in Fig. 7, an increased probability of higher conductance substates (qualitatively consistent with an increased N_{app}) would have resulted for PA IX at the same voltage as for PA V. Note that in another couple of peptaibols also, presenting either a Trpol or a Pheol C-terminal, the 19-residue long trichorzianins TB IIIc and TB VII, respectively (see Fig. 1), a lower oligomerization state was also observed with the former [19]. The reduced number of monomers per aggregate observed with PA V is also consistent with the decreased single-channel conductances induced by the same analogue, and could reflect the higher steric hindrance of Trpol as compared to Pheol. Indeed, in the helical wheel representation of trichorzins, these C-terminal amino alcohols lie quite close to the inter-helical hydrophobic contact zone, and thus could result in bundle distortion. Note that, contrasting with the present study, slightly increased single-channel conductance amplitudes were observed with trichorzianins TB IIIc and TB VII [19]. However, in the latter case, the amino alcohol has a quite different location in the helical wheel, due to an additional – and proximal – negatively charged residue (Glu18).

Finally, from a kinetic point of view, the larger hysterisis observed for PA V on I/V curves are in favour of longer channel durations for the Trpol analogue in agreement with the lifetime values determined for the different open states in single-channel experiments (Table 2). These results emphasize the role of Trpol in the stabilization of conducting aggregates. This effect was more significant with the two previously studied 19-residue trichorzianins mentioned above [19] and was also described in a modified gramicidin in which the four Trp residues replacement by phenylalanines resulted in shorter mean lifetime of the open channel [35]. Presumably, as demonstrated in a subsequent molecular modelling study on gramicidin in the presence of water and explicit bilayer [36], hydrogen bonds formation between indole groups and polar heads would be the main determinant in this modulation of channel lifetime. A stereochemical analysis of classical H-bonds donors and acceptors in refined protein structures had previously shown that the nitrogen atom in the indole ring of tryptophan is an unambiguous donor [37]. Given the high frequency of occurrence of aromatic residues in interfacial rings, e.g. in porins [38], and the higher tryptophan content of membrane protein (3.3%) compared to soluble proteins (1.2%) [39], our results argue that this amino acid may have, in addition to a structural role as anchor [40], a functional role in channel open-state stabilization.

Acknowledgements

We thank Christophe Goulard for skillful technical assistance. This work was supported by the ‘‘Groupement de Recherches Peptides et Protéines Amphipathiques’’ (GDR 1153, CNRS).

References

[1] D. Duval, S. Rebuffat, C. Goulard, Y. Prigent, M. Becchi, B. Bodo, J. Chem. Soc., Perkin Trans. 1 (1997) 2147–2153.
[2] R.C. Pandey, J.C. Cook Jr., K.L. Rinehart Jr., J. Am. Chem. Soc. 99 (1977) 8469–8483.
[3] B. Bodo, S. Rebuffat, M. El Hajji, D. Davoust, J. Am. Chem. Soc. 107 (1985) 6011–6017.
[4] G. Jung, W.A. König, D. Leibfritz, T. Ooka, K. Janko, G. Boheim, Biochim. Biophys. Acta 433 (1976) 164.
[5] A. Iida, M. Okuda, S. Uesato, Y. Takaishi, T. Shingu, M. Morita, T. Fujita, J. Chem. Soc., Perkin Trans. 1 (1990) 3249–3255.
[6] S. Rebuffat, Y. Prigent, C. Auvin-Guette, B. Bodo, Eur. J. Biochem. 201 (1991) 661–674.
[7] S. Rebuffat, M. El Hajji, P. Hennig, D. Davoust, B. Bodo, Int. J. Peptide Protein Res. 34 (1989) 200–210.
[8] K.L. Rinehardt, L.A. Gaudioso, M.L. Moore, R.C. Pandey, J.C. Cook, M. Barber, R.D. Sedgwick, R.S. Bordoli, A.N. Tyler, B.N. Green, J. Am. Chem. Soc. 103 (1981) 6517–6520.
[9] S. Rebuffat, C. Goulard, B. Bodo, J. Chem. Soc., Perkin Trans. 1 (1995) 1849–1855.
[10] S. Rebuffat, S. Hlimi, Y. Prigent, C. Goulard, B. Bodo, J. Chem. Soc., Perkin Trans. 1 (1996) 2021–2027.
[11] C. Auvin-Guette, S. Rebuffat, Y. Prigent, B. Bodo, J. Am. Chem. Soc. 114 (1992) 2170–2174.
[12] C. Auvin-Guette, S. Rebuffat, I. Vuidepot, M. Massias, B. Bodo, J. Chem. Soc., Perkin Trans. 1 (1993) 249–255.
[13] T. Fujita, S. Wada, A. Iida, T. Nishimura, M. Kanai, N. Toyama, Chem. Pharm. Bull. 42 (1994) 489–494.

[14] G. Bauman, P. Mueller, J. Supramol. Struct. 2 (1974) 538–557.
[15] G. Boheim, J. Membr. Biol. 19 (1974) 277–303.
[16] M.P.S. Sansom, Prog. Biophys. Mol. Biol. 55 (1991) 136–235.
[17] D.S. Cafiso, Annu. Rev. Biophys. Biomol. Struct. 23 (1994) 141–165.
[18] G. Molle, H. Duclohier, G. Spach, FEBS Lett. 224 (1987) 208–212.
[19] H. Duclohier, G. Molle, G. Spach, Biochim. Biophys. Acta 987 (1989) 133–134.
[20] S. Rebuffat, H. Duclohier, C. Auvin-Guette, G. Molle, G. Spach, B. Bodo, FEMS Microbiol. Immunol. 105 (1992) 151–160.
[21] M. Lucaciu, S. Rebuffat, C. Goulard, H. Duclohier, M. Molle, B. Bodo, Biochem. Biophys. Acta 1323 (1997) 85–96.
[22] M. Montal, P. Mueller, Proc. Natl. Acad. Sci. USA 69 (1972) 3561–3566.
[23] W. Hanke, C. Methfessel, U. Wilmsen, G. Boheim, Biochem. Bioenerg., J. 12 (1984) 329–336.
[24] S.S. Lehrer, Biochem. 10 (1971) 3254–3263.
[25] T. Le Doan, M. El Hajji, S. Rebuffat, M.R. Rajesvari, B. Bodo, Biochim. Biophys. Acta. 858 (1986) 1–5.
[26] M. El Hajji, S. Rebuffat, T. Le Doan, G. Klein, M. Satre, B. Bodo, Biochim. Biophys. Acta. 978 (1989) 97–104.
[27] J.N. Weinstein, S. Yoshikami, P. Henkart, R. Blumenthal, W.A. Hagins, Science 195 (1977) 489–492.
[28] J. Hall, I. Vodyanoy, T. Balasubramanian, R. Marshall, Biophys. J. 45 (1984) 233–247.
[29] G. Esposito, J.A. Carver, J. Boyd, I.D. Campbell, Biochem. 26 (1987) 1043–1050.
[30] A.A. Yee, R. Babiuk, J.D.J. O'Neil, Biopolymers 36 (1995) 781–792.
[31] J.C. Franklin, J.F. Ellena, S. Jayasinghe, L.P. Kelsh, D.S. Cafiso, Biochem. 33 (1994) 4036–4045.
[32] G. Boheim, G. Irmsher, G. Jung, Biochim. Biophys. Acta 507 (1978) 485–506.
[33] G. Boheim, S. Gelfert, G. Jung, G. Menestrina, in: K. Yagi, B. Pullman (Eds.), Ion Transport Through Membranes, Academic Press Japan, Tokyo, 1987, pp. 131-145.
[34] G. Molle, H. Duclohier, S. Julien, G. Spach, Biochim. Biophys. Acta 1064 (1991) 345–349.
[35] F. Heitz, G. Spach, Y. Trudelle, Biophys. J. 36 (1982) 87–89.
[36] T. Woolf, B. Roux, Proc. Natl. Acad. Sci. USA 91 (1994) 11631–11635.
[37] J.A. Ippolito, R.S. Alexander, D.W. Christianson, J. Mol. Biol. 215 (1990) 457–471.
[38] S.W. Cowan, T. Schirmer, G. Rummel, M. Steiert, R. Ghosh, R.A. Pauptit, J.N. Jansonius, J.P. Rosenbusch, Nature 358 (1992) 727–733.
[39] G. Von Heijne, EMBO J. 5 (1987) 3021–3027.
[40] M. Schiffer, C.H. Chang, F.J. Stevens, Protein Eng. 5 (1992) 213–214.